Medical Engineering and Physics 53 (2018) 32–38

Contents lists available at ScienceDirect

Medical Engineering and Physics

journal homepage: www.elsevier.com/locate/medengphy

A finite element modeling study of peripheral nerve recruitment by percutaneous tibial nerve stimulation in the human lower leg

Christopher W. Elder[a], Paul B. Yoo[a,b,*]

[a] Institute of Biomaterials and Biomedical Engineering, University of Toronto, 164 College Street, Toronto, Ontario M5S 3G9, Canada
[b] Department of Electrical and Computer Engineering, University of Toronto, 10 King's College Road, Toronto, Ontario M5S 3G4, Canada

ARTICLE INFO

Article history:
Received 13 July 2017
Revised 30 December 2017
Accepted 3 January 2018

Keywords:
Finite element model
Overactive bladder
Percutaneous tibial nerve stimulation
Saphenous nerve
Neuromodulation

ABSTRACT

Percutaneous tibial nerve stimulation (PTNS) is a clinical therapy for treating overactive bladder (OAB), where an un-insulated stainless steel needle electrode is used to target electrically the tibial nerve (TN) in the lower leg. Recent studies in anesthetized animals not only confirm that bladder-inhibitory reflexes can be evoked by stimulating the TN, but this reflex can also be evoked by stimulating the adjacent saphenous nerve (SAFN). Although cadaver studies indicate that the TN and major SAFN branch(es) overlap at the location of stimulation, the extent to which SAFN branches are co-activated is unknown. In this study, we constructed a finite element model of the human lower leg and applied a numeric axon model (MRG model) to simulate the electrical recruitment of TN and SAFN fibers during PTNS. The model showed that up to 80% of SAFN fibers (located at the level of the needle electrode) can be co-activated when electrical pulses are applied at the TN activation threshold, the standard therapeutic amplitude. Both the location of the inserted electrode and stimulation amplitude were important variables that affected the recruitment of SAFN branches. This study suggests further work is needed to investigate the potential therapeutic effects of SAFN stimulation in OAB patients.

1. Introduction

Percutaneous tibial nerve stimulation (PTNS) is a minimally-invasive electrical neuromodulation therapy that has been shown to treat effectively symptoms of overactive bladder (OAB) [1–3]. Although the therapeutic mechanism is unknown, the historical origins of PTNS suggest that electrical activation of tibial nerve (TN) fibers is a necessary requirement for treating OAB symptoms. This idea is supported by preclinical studies in anesthetized animals, which show that TN stimulation – using an implanted nerve cuff electrode, for example – can evoke bladder-inhibitory responses that persist after the stimulus has been turned off. This prolonged inhibitory effect is depicted by significant increases in the bladder capacity and also by changes in the time interval between successive bladder contractions [4–7]. Experimental studies consistently show that large stimulation amplitudes (2 to 6 times the foot motor threshold) and specific stimulation frequencies (between 5 Hz and 20 Hz) are needed to evoke these responses.

However, clinical studies show that the therapeutic effects of PTNS in OAB patients can vary considerably, with treatment success ranging between 37% and 81% [8]. Studies investigating the functional changes in response to TN stimulation also exhibit some degree of variability among human subjects. Mang el al. recently showed that increases in bladder capacity can be achieved by transcutaneous stimulation of the plantar foot surface using large stimulation amplitudes ($\geq$ 4 times the foot motor threshold) [9]. Amarenco et al. reported similar increases in bladder capacity but with low-amplitude stimuli (below the foot motor threshold) applied near the medial malleolus [10]. Fjorback et al. on the other hand, reported that PTNS altogether fails to increase bladder capacity in patients with neurogenic bladder dysfunction [11]. Taken together, it is unclear how bladder-inhibitory responses evoked by TN stimulation – such as increases in bladder capacity – are related to the clinical effects of PTNS therapy.

As an alternative approach, we have begun investigating the idea that the saphenous nerve (SAFN) contributes to the therapeutic effects of PTNS therapy. It is known that the SAFN provides cutaneous sensory innervation to the medial aspect of the lower leg, and therefore anatomically overlaps with the location at which the PTNS electrode is inserted. Human cadaver studies show that the main trunk of the SAFN, can provide one or more posterior branches cephalad to the medial malleolus [12–14]. In addition, there is emerging preclinical evidence that shows electrical

Abbreviations: OAB, overactive bladder; PTNS, percutaneous tibial nerve stimulation; TN, tibial nerve; SAFN, saphenous nerve; FEM, finite element model.

* Corresponding author at: Institute of Biomaterials and Biomedical Engineering, University of Toronto, 164 College Street, Rosebrugh Bldg. Rm. 407, Toronto, Ontario, Canada, M5S 3G9.
E-mail address: paul.yoo@utoronto.ca (P.B. Yoo).

https://doi.org/10.1016/j.medengphy.2018.01.004
1350-4533/

stimulation of the SAFN can evoke bladder-inhibitory responses. In urethane-anesthetized rats, Moazzam and Yoo showed that electrical stimulation of the SAFN between 10 Hz and 20 Hz (using an implanted nerve cuff electrode) elicits significant increases in both bladder capacity and the time interval between successive bladder contractions [15]. Not only were the inhibitory effects of SAFN stimulation comparable to that of TN stimulation when tested in the same experimental setup [6], but the stimulation amplitude used to evoke the SAFN-mediated responses was also notably smaller (25 μA for SAFN vs. 150 μA for TN).

In light of these findings, we investigated the extent to which the SAFN (or parts thereof) can be electrically co-activated during PTNS. We implemented a computational model that simulated percutaneous needle stimulation in a human lower leg, and tested the hypothesis that PTNS electrically activates (via stimulation spillover) one or more branches of the SAFN. We measured the relative activation of the TN and SAFN while varying (1) the type of needle electrode used (insulated vs. un-insulated), (2) the location of electrode within the lower leg, and (3) the amplitude of the stimulus current applied through the needle electrode. Preliminary results of this study were presented in abstract form [16].

2. Materials and methods

A two-step computational approach was used to simulate electrical activation of the TN and SAFN by a percutaneous needle electrode. First, a finite element model (FEM) of the human lower leg was used to solve for the extracellular potentials generated along individual axons that were centered within each nerve. This was followed by the use of quantitative methods to predict the generation of action potentials by individual axons. A similar methodology for computationally modeling nerve activation has been described previously [17].

2.1. Finite element model

The FEM was based on a cross sectional image of a human lower leg [18], located proximal to the medial malleolus. The visible boundaries of anatomical structures were traced (Adobe Illustrator, Adobe Systems Inc), and the total area of the cross-sectional image was scaled in proportion to the known area of the flexor hallucis longus muscle (approximately 5 cm^2) [19]. The digitized image was imported into a finite element software (COMSOL Multiphysics, Comsol Inc) and extruded (length = 20 cm) along the longitudinal axis (Fig. 1) to create a 3-dimensional model. The extrusion length was selected to ensure minimal error (< 4%) in the simulated extracellular potential due to the imposed boundary conditions. Based on gross dissections conducted in human cadavers (approved by the University of Toronto Research Ethics Board), we modeled the TN as a single monofascicular nerve with a diameter of 3 mm. Due to the diffuse sensory innervation pattern, the SAFN was modeled as five individual branches (each with a diameter of 1 mm) that were evenly distributed across the subcutaneous layer (Fig. 1a). All nerves consisted of an endoneurium that was encircled by perineurium (50 μm thickness) and epineurium (200 μm thickness) layers [20–22]. As shown in Table 1, each component of the model was assigned a conductivity value cited from existing literature [17,21,23].

Percutaneous electrical nerve stimulation was modeled using either an un-insulated stainless steel needle electrode (cylinder, diameter = 220 μm, length = 3 cm) or as an insulated needle electrode in which the active tip was approximated by a point source (cube = 220 μm × 220 μm × 220 μm). In either case, the electrode was set as the cathode (e.g., I = −0.2 mA) and the distal surface of the FEM was set as the electrical ground. The electrical ground emulated the return electrode that is clinically placed on the sole of the foot. Solving the FEM yielded extracellular potential values along each nerve (Fig. 2a). Since the model is assumed to be a linear system, the extracellular voltages generated by higher or lower stimulation amplitudes were simply scaled with respect to the extracellular potentials obtained at I = 0.2 mA.

Table 1
Material properties of the finite element model.

Material	Conductivity (S/m)
Bone	0.02
Blood	0.7
Fat	0.03
Skin	0.0014
Radial muscle	0.11
Axial muscle	0.33
Epineurium	0.0826
Perineurium	0.0021
Radial endoneurium	0.0826
Axial endoneurium	0.517
Connective tissue	0.15
Needle electrode	4.032×10^6

First, the accuracy of our FEM was tested by determining the strength-distance relationship, which related the TN activation threshold to the nerve-electrode distance. The needle was displaced in 0.1 cm increments following a straight path moving away from the TN, as shown in Fig. 1 (range = 0–1.7 cm). This procedure was repeated for both an insulated and un-insulated needle electrode, and subsequently compared with data reported in the literature. Next, clinical PTNS was simulated by varying the location of the needle electrode within the cross-sectional image of the lower leg. In accordance with clinical guidelines (Urgent PC, Cogentix Medical Inc), the needle was initially placed 2 cm posterior to the posterior-medial edge of the tibia, at a depth of 2 cm, and at an angle of 60% to the sagittal plane. This corresponded to an approximate distance of 1.73 cm between the needle electrode tip and the skin surface (Fig. 1). Simulation of PTNS was repeated at multiple locations to account for both inter-patient and operator variability. This region was defined by a 5 × 10 grid (dimensions = 1 cm × 2 cm), where the center of each pixel corresponded to the tip of the needle electrode.

2.2. Numerical estimation of nerve activation

Using the extracellular voltage obtained from the FEM, electrical activation of single myelinated nerve fibers located within the TN and SAFN was predicted by (1) determining the activating function (AF) and (2) using the MRG double cable axon model. The AF was obtained by computing the second spatial difference of the extracellular potential at each node of Ranvier along individual axons [24]; while the MRG model was used to determine numerically the nerve activation threshold [25–27]. All nerve activation threshold values obtained from the MRG model were based on single electrical stimulus pulses with a 200 μs pulse width, as used during clinical PTNS. Each axon within the TN and SAFN were assumed to have a diameter of 12 μm (1.2 mm inter-nodal distance), which is consistent with the large diameter mammalian myelinated axons [28,29]. The extracellular potential was sampled at 0.5 mm intervals, linearly interpolated along the axon, and used in calculating the AF and determining the MRG-derived nerve activation threshold (Fig. 2).

3. Data analysis

The relative activation of TN and SAFN fibers was quantified by two different methods. First, the AF was used to provide an estimate of the relative excitability of each nerve, and is solely dependent on the distances between each respective nerve and the

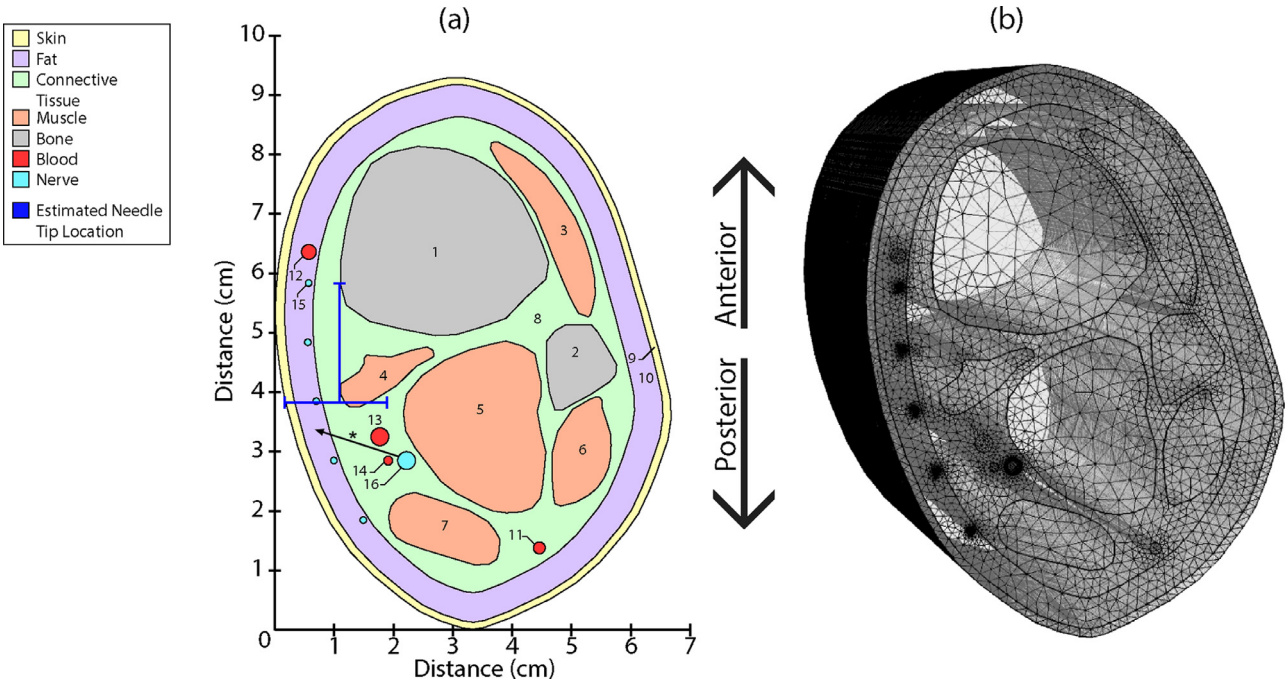

Fig. 1. (a) Finite element model cross section (1-tibia, 2-fibula, 3-fibularis tertius, 4-flexor digitorum longus, 5-flexor hallucis longus, 6-fibularis brevis, 7-soleus, connective tissue, 9-skin, 10-cutaneous fat, 11-small saphenous vein, 12-greater saphenous vein, 13-posterior tibial artery, 14-posterior tibial vein, 15-saphenous nerve branch, 16-tibial nerve). The estimated placement of the needle electrode – as described clinically – is indicated by the horizontal and vertical bars (2 cm posterior to the tibia and 1.73 cm deep) (b) Meshed extrusion of the finite element model. [*, path of needle displacement for strength-distance analysis].

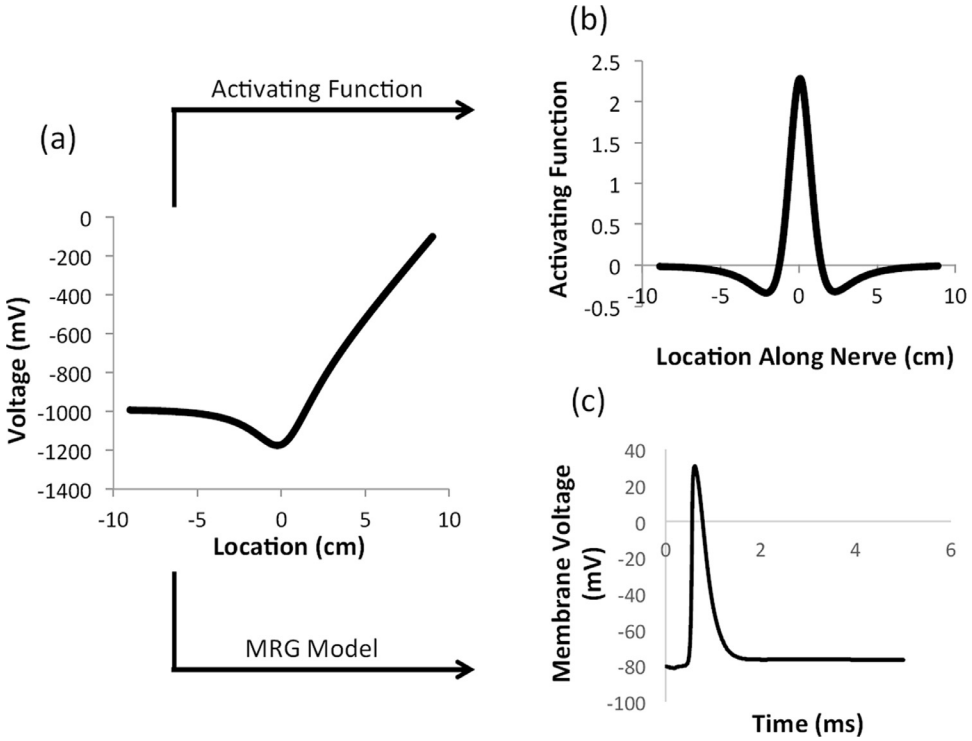

Fig. 2. (a) Voltage profile extracted from the center of the tibial nerve along the length of the FEM extrusion. Considered to be the extracellular voltage profile of an axon. (b) Activating function calculated using the voltage profile, where neural excitability is proportional to the maximum value. (c) Action potential predicted by the MRG model in response to the voltage profile applied for 200 μs.

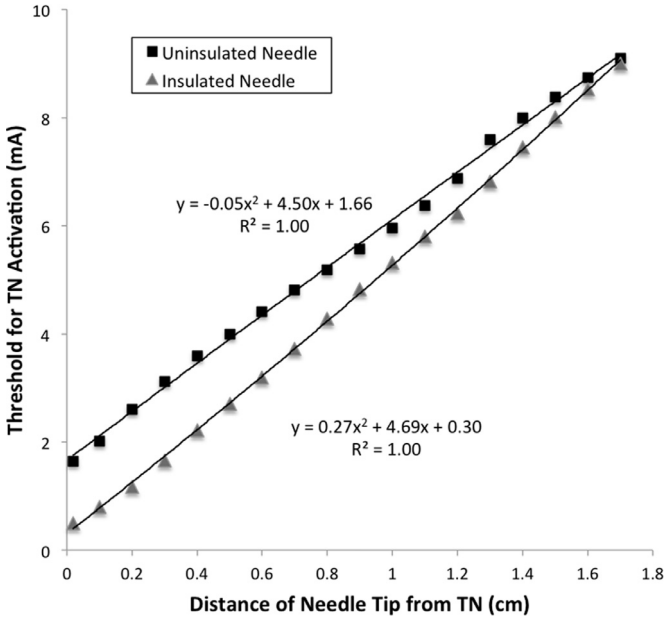

Fig. 3. Strength-distance relationships displaying current amplitude required for tibial nerve activation at varying electrode-to-nerve distances for both an insulated and un-insulated needle. The electrode tip was displaced from the tibial nerve along a straight path (arrow indicated with asterisk, refer to Fig. 1a). Thresholds were determined using the MRG model.

electrode tip. A selectivity ratio (SR) was defined as the ratio of the AF between the TN and a single SAFN branch:

$$SR = \frac{\max(\text{AF of TN})}{\max(\text{AF of SAFN branch})} \quad (1)$$

A SR value of unity indicates equal activation of TN and SAFN; while any value greater than unity denotes greater selective activation of the TN. The SR was determined by using the maximum value of the AF that was calculated along each nerve.

The second method quantified the co-activation of the SAFN during PTNS by determining the number of SAFN branches that were activated at various stimulation amplitudes. This analysis was performed at specific multiples of the threshold for TN activation (0.5T, 0.8T, 1T, 2T and 4T) – which were predicted by the MRG model – and was repeated for all 50 electrode tip locations within the 5 × 10 grid.

4. Results

4.1. Strength–Distance Relationship: validation of computer model

Our model showed that the threshold for TN activation increased rapidly as the electrode tip was displaced farther away from the nerve (Fig. 3, distance = 0 cm–1.7 cm): 1.6 mA–5.9 mA for the un-insulated needle, and 0.3 mA– 5.3 mA for the insulated needle. The path of needle tip displacement is indicated by the arrow in Fig. 1a. Differences in nerve activation threshold between the two types of needle electrodes were notably greater at shorter electrode-to-TN distances. And, as shown in Figs. 4a and 5a, the larger threshold amplitudes needed with the uninsulated needle electrode can be attributed to a greater dispersion of stimulus current within the subcutaneous tissue. The strength-distance properties of this model are consistent with the literature [30–33].

4.2. SAFN activation with an uninsulated needle electrode (PTNS)

Our computational simulations showed that electrical activation of SAFN branches can occur when using an uninsulated needle electrode. Selective activation of either the TN or SAFN – as predicted by the activating function – was strongly dependent on the location of the electrode within the lower leg. With the electrode placed according to clinical guidelines for PTNS (location 3C in grid, Fig. 4b), the corresponding SR values indicated that SAFN branches II, III and IV have lower activation thresholds than the TN. As the electrode was displaced in the posterior direction – for example, between grid points 1C and 8C in SAFN II – an increase in the SR (> 1) indicated that the activation threshold of the TN was lower, relative to SAFN II. The proximity of the uninsulated electrode shaft to any of the SAFN branches also affected the SR value. As shown in Fig. 4b (SAFN IV), the uninsulated needle happened to overlap with SAFN IV and, as a result, the SR values along row 8 are all less than unity (SR = 2.6×10^{-3} to 9.7×10^{-3}). In this particular example, SAFN IV exhibits a lower activation threshold than the TN at every location within the grid (SR < 1).

Electrical activation of the SAFN was also confirmed when predicting neural activation with the MRG model. As shown in Fig. 4c, simulation of PTNS applied at 1T (i.e., TN activation threshold) showed electrical activation of at least one SAFN branch at every location within the 5 × 10 grid. Co-activation of 80% of the SAFN branches occurred when the needle electrode was placed approximately 1–1.2 cm anterior to the TN (rows 1–2, closer to the posterior edge of the tibia); while 20–60% recruitment of SAFN branches occurred when the electrode was positioned in more posterior locations (rows 5–10). Increasing the PTNS amplitude (2T and 4T) resulted in more electrode locations (approximately 50% of the grid) at which electrical activation of all SAFN branches (100%) was predicted. It is interesting to point out that sub-threshold PTNS (< 1T) could also result in up to 80% activation of SAFN branches.

4.3. Effects of using an insulated needle electrode

Switching the electrode to an insulated needle resulted in a noticeable trend towards more preferential activation of the TN, rather than the SAFN branches. If we compare the SR of each pixel between the uninsulated (Fig. 4b) and insulated (Fig. 5b) electrodes, there is a notable decrease in the relative threshold for activating the TN, relative to the SAFN. For example, in the case of SAFN branch I, not only did the total number of electrode locations that yielded an SR value greater than unity increase from 40 (Fig. 4b) to 46 (Fig. 5b), but the average SR value across the entire 5 × 10 grid exhibited a 2-fold increase (Fig. 6). The average increase in SR also doubled with respect to SAFN branches II, and V; whereas much larger increases (40-fold) were obtained with respect to SAFN branches III and IV.

Consistent with the above analysis, the MRG model also predicted a decrease in number of SAFN branches that were co-activated during percutaneous stimulation. As shown in Fig. 5c (dark grey pixels), there were a notable number of electrode locations that failed to activate any SAFN branch. For example, when compared to stimulation with an uninsulated needle at 1T (Fig. 4c), there was a 36% decrease in the number of grid points at which co-activation of SAFN branches occurred. Even at larger amplitudes (2T and 4T), there were 20% and 10% fewer grid points that showed SAFN branch co-activation, respectively. As shown in Fig. 7, selective activation of only the TN was achieved when the tip of the insulated needle was within 0.28 ± 0.24 cm of the target nerve at 1T. At larger amplitudes (2T and 4T), the maximum nerve-to-electrode distances that achieved selective TN activation were 0.12 ± 0.11 cm and 0.02 ± 0.06 cm, respectively. The significant difference in the

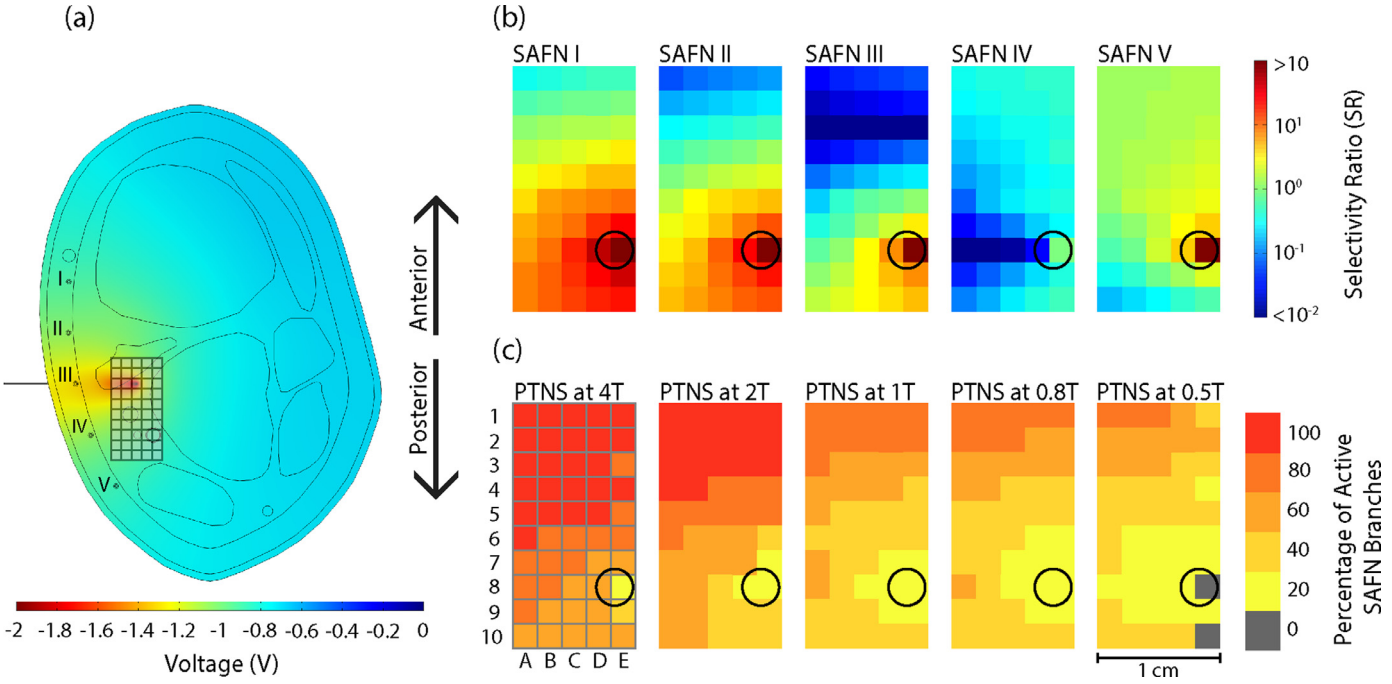

Fig. 4. (a) Cross section of the voltage profile from the center of the FEM extrusion, for a stimulus applied with an un-insulated needle electrode. The 5 × 10 array of 0.2 cm spaced electrode tip locations used for analysis is highlighted. The saphenous nerve branches are labeled I–V and the tibial nerve is indicated by the black circle (intersects grid points 7D–E, 8D–E, and 9D–E). (b) Selectivity ratio calculated for each saphenous nerve branch at each electrode location, for an un-insulated needle electrode. (c) Percentage of SAFN branches found to be active by the MRG model when stimulating the TN at varying amplitudes with an un-insulated needle electrode. The location of each grid point within the array is defined by the row number and column letter (e.g., needle tip location in Fig. 4(a) = 3C).

nerve-to-electrode distance between 1T and 4T (Fig. 7, $p < 0.05$) suggests that selective activation of the TN becomes more difficult when the stimulation amplitude exceeds 2T. It is particularly interesting to point out that activation of at least one SAFN branch is observed even without TN activation (amplitude < 1T), when the electrode tip is located at least 0.50 ± 0.36 cm (0.5T) and 0.36 ± 0.3 cm (0.8T) away from the TN.

5. Discussion

In this study, a computational model of the human lower leg was constructed to investigate the electrical recruitment of SAFN branches during clinical PTNS. The rationale for pursuing this work was based in part by the neuroanatomy of peripheral nerves (namely, the TN and SAFN branches) in the lower leg, and also by our recent pre-clinical animal studies that show a bladder-inhibitory reflex evoked by SAFN stimulation [15]. Our model showed that when PTNS is applied at the TN activation threshold (1T) – which is analogous to the foot motor threshold used in OAB patients – up to 80% of SAFN branches located at the level of the needle electrode can be electrically recruited. We found that the degree of SAFN activation – between 20% and 80% of SAFN branches – was dependent on both the location of the inserted needle electrode and the stimulation amplitude. Our results particularly underscore that fact that using an 'uninsulated' needle electrode facilitates stimulus spillover into the surrounding SAFN branches. Similarities between the strength-distance curves (Fig. 3) generated by our computational model and those reported in the literature [30–33], suggest this study yielded accurate approximations of TN and SAFN branch recruitment.

Since the seminal work by McGuire et al. [34], the scientific and clinical literature attributes PTNS therapy as a functional outcome of electrically activating the tibial nerve. Unlike sacral neuromodulation, the therapeutic process takes at least several weeks before patients report any changes in OAB symptoms, and the therapeutic effects persist in between weekly stimulation sessions. Based on findings from preclinical studies in anesthetized animals [4–6], it is reasonable to understand the clinical effects of PTNS as being linked with the repeated activation of a prolonged bladder-inhibitory reflex. However, it is also important to consider that the stimulation amplitude used in patients is commonly set at or just below the foot motor threshold. Despite the relatively consistent manner in which the TN is electrically activated, the percentage of patients that respond positively to 12 weeks of PTNS appear to vary considerably, between 37% and 82% [8]. The mechanism(s) of PTNS therapy remain unknown.

Flexion of the hallux or sensations radiating along the sole of the foot are widely accepted physiological biomarkers that determine the therapeutic stimulation amplitude used in patients. As a consequence, attributing part of the therapeutic effects to the unintended activation of SAFN fibers may not appear logical. In fact, tingling in the leg and discomfort at the needle site (presumably due to SAFN fiber activation) are considered adverse events [35]. But it is interesting that patients anecdotally state they can feel sensation around the needle electrode during stimulation and some may experience this sensation expand in a rostral direction (personal communication with Dr. Scott MacDiarmid). If the patient indicates discomfort at the needle site, the practitioner may push the needle deeper or move to another insertion site. This type of adjustment is consistent with our model (Fig. 3b), which shows that the threshold for activating a SAFN branch is significantly lower than the TN when (1) the electrode tip is closer to the skin surface and (2) the shaft of the needle is in contact with a SAFN branch. Under these particular conditions, activation of SAFN branch(es) may cause discomfort before the TN is electrically recruited.

It is important to note that our model was constructed to characterize accurately the electrical recruitment of TN and SAFN fibers

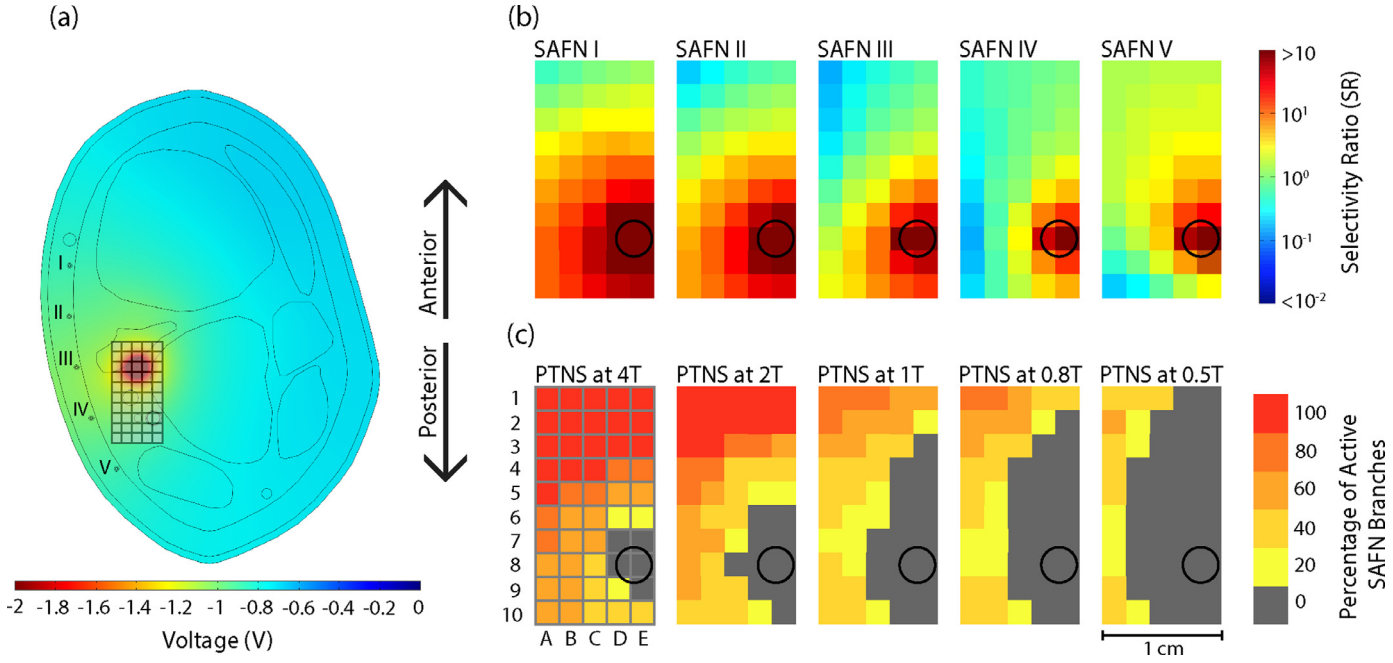

Fig. 5. (a) Cross section of the voltage profile from the center of the FEM extrusion, for a stimulus applied with an insulated needle electrode. The 5 × 10 array of 0.2 cm spaced electrode tip locations used for analysis is highlighted. The saphenous nerve branches are labeled I–V and the tibial nerve is indicated by the black circle (intersects grid points 7D–E, 8D–E, and 9D–E). (b) Selectivity ratio calculated for each saphenous nerve branch at each electrode location, for an insulated needle electrode. (c) Percentage of SAFN branches found to be active by the MRG model when stimulating the TN at varying amplitudes with an insulated needle electrode. The location of each grid point within the array is defined by the row number and column letter (e.g., needle tip location in Fig. 5(a) = 3C).

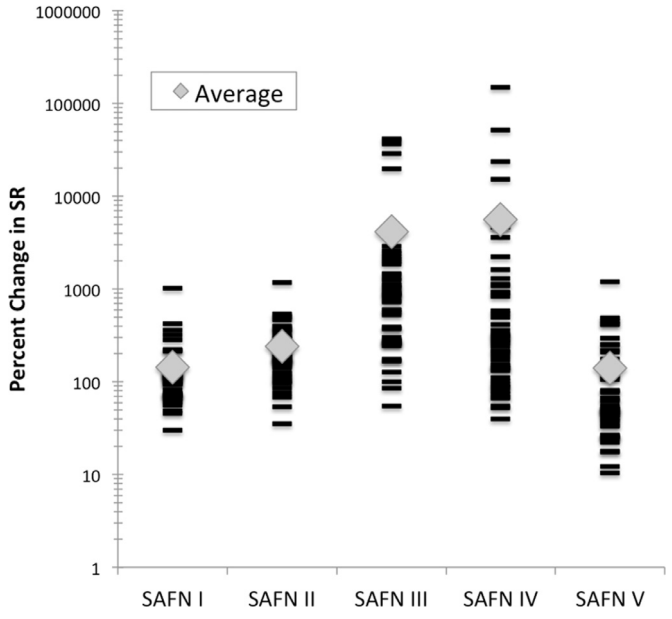

Fig. 6. The percent change in the selectivity ratio (SR), when switching from an un-insulated to an insulated needle, indicated an increase in the excitability of the tibial nerve relative to each saphenous nerve branch. The percent change in SR was calculated as (insulated SR - un-insulated SR)/un-insulated SR, for each of the 50 pairs of electrode locations within the 5 × 10 array (refer to Figs. 4b and 5b). The average percent change value is indicated (grey diamond) for each saphenous nerve branch.

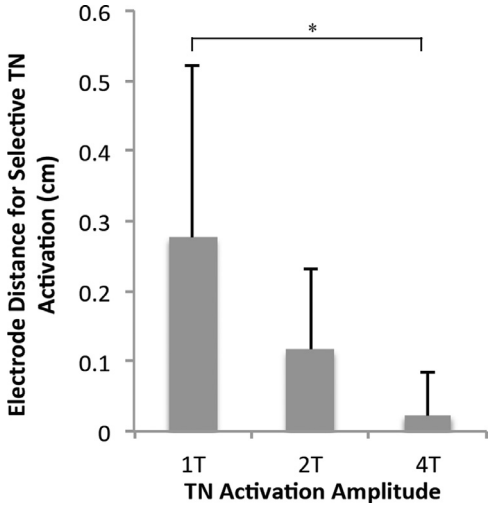

Fig. 7. Comparison of the nerve-to-electrode tip distances at which selective tibial nerve (TN) activation was achieved with PTNS applied at 1T, 2T, and 4T (refer to Fig. 5c). The average distances achieved at each stimulus amplitude were compared by performing a one-way ANOVA followed by a Tukey–Kramer multi-comparison. [*, $p < 0.05$].

at the needle insertion site. Within this coronal slice of the lower leg, we showed that selective electrical activation of the TN by PTNS is very difficult, even with an insulated needle electrode. Nonetheless, the current model provides a template that can be modified to further investigate the nerve recruitment properties of PTNS. These include the different physical dimensions of the lower leg, variable size of individual components and body fat composition, and higher electrical conductivity values that can be used to approximate the effects of edema (e.g., venous insufficiency). Complex three dimensional models of the lower leg, constructed from multiple cross-sectional images along the entire length of the lower leg, may enable more accurate simulations of peripheral nerve activation.

6. Conclusion

By constructing a finite element model of the human lower leg, we computationally showed the propensity of PTNS for electrically

activating one or more SAFN branches. Combined with preclinical evidence of a bladder-inhibitory reflex evoked by SAFN stimulation, the results of this study provide a potential explanation as to how 'low-amplitude' PTNS can elicit strong therapeutic effects in some OAB patients. It further suggests the possibility of co-activating the SAFN trunk (e.g., above or below the knee) to further improve the clinical effectiveness of PTNS. Further clinical work is needed to investigate the therapeutic effects of SAFN stimulation.

Competing interests

Dr. Paul Yoo (assigned to the University of Toronto) has filed patent applications that describe the clinical use of saphenous nerve stimulation.

Funding

This work was supported by University of Toronto Connaught Innovation Award, and the Canadian Institutes of Health Research (CIHR) [grant number 345331].

Ethical approval

Ethical approval for the human cadaver study was given by the University of Toronto, Office of Research Ethics. The protocol reference number for approval was 32318.

Supplementary materials

Supplementary material associated with this article can be found, in the online version, at doi:10.1016/j.medengphy.2018.01.004.

References

[1] Peters KM, Carrico DJ, Wooldridge LS, Miller CJ, MacDiarmid SA. Percutaneous tibial nerve stimulation for the long-term treatment of overactive bladder: 3-year results of the STEP study. J Urol 2013;189:2194–201. doi:10.1016/j.juro.2012.11.175.

[2] Van Der Pal F, Van Balken MR, Heesakkers JPFA, Debruyne FMJ, Bemelmans BLH. Percutaneous tibial nerve stimulation in the treatment of refractory overactive bladder syndrome: is maintenance treatment necessary? BJU Int 2006;97:547–50. doi:10.1111/j.1464-410X.2006.06055.x.

[3] MacDiarmid SA, Peters KM, Shobeiri SA, Wooldridge LS, Rovner ES, Leong FC, et al. Long-term durability of percutaneous tibial nerve stimulation for the treatment of overactive bladder. J Urol 2010;183:234–40 doi:10.1016/j.juro.2009.08.160.

[4] Tai C, Shen B, Chen M, Wang J, Roppolo JRR, de Groat WCC. Prolonged post-stimulation inhibition of bladder activity induced by tibial nerve stimulation in cats. Am J Physiol Ren Physiol 2011;300:F385–92 doi:10.1152/ajprenal.00526.2010.

[5] Su X, Nickles A, Nelson DE. Comparison of neural targets for neuromodulation of bladder micturition reflex in the rat. Am J Physiol Ren Physiol 2012;303:F1196–206 doi:10.1152/ajprenal.00343.2012.

[6] Kovacevic M, Yoo PB. Reflex neuromodulation of bladder function elicited by posterior tibial nerve stimulation in anesthetized rats. Am J Physiol Physiol 2015;308:F320–9. doi:10.1152/ajprenal.00212.2014.

[7] Moazzam Z, Duke AR, Yoo PB. Inhibition and excitation of bladder function by tibial nerve stimulation using a wirelessly powered implant: an acute study in anesthetized cats. J Urol 2016;196:926–33. doi:10.1016/j.juro.2016.04.077.

[8] Burton C, Sajja A, Latthe PMPM, Sajja A, Latthe PMPM. Effectiveness of percutaneous posterior tibial nerve stimulation for overactive bladder: a systematic review and meta-analysis. Neurourol Urodyn 2012;31:1206–16 doi:10.1002/nau.

[9] Chen ML, Chermansky CJ, Shen B, Roppolo JR, de Groat WC, Tai C. Electrical stimulation of somatic afferent nerves in the foot increases bladder capacity in healthy human subjects. J Urol 2014;191:1009–13 doi:10.1016/j.juro.2013.10.024.

[10] Amarenco G, Ismael SS, Even-Schneider A, Raibaut P, Demaille-Wlodyka S, Parratte B, et al. Urodynamic effect of acute transcutaneous posterior tibial nerve stimulation in overactive bladder. J Urol 2003;169:2210–15. doi:10.1097/01.ju.0000067446.17576.bd.

[11] Fjorback MV, Van Rey FS, Van der Pal F, Rijkhoff NJM, Petersen T, Heesakkers JP. Acute urodynamic effects of posterior tibial nerve stimulation on neurogenic detrusor overactivity in patients with MS. Eur Urol 2007;51:462–4 doi:10.1016/j.eururo.2006.07.024.

[12] Wilmot VV, Evans DJ. Categorizing the distribution of the saphenous nerve in relation to the great saphenous vein. Clin Anat 2013;26:531–6. doi:10.1002/ca.22168.

[13] Mercer D, Morrell NT, Fitzpatrick J, Silva S, Child Z, Miller R, et al. The course of the distal saphenous nerve: a cadaveric investigation and clinical implications. Iowa Orthop J 2011;31:231–5.

[14] Veverková L, Jedlicka V, Vlcek P, Kalac J. The anatomical relationship between the saphenous nerve and the great saphenous vein. Phlebology 2011;26:114–18. doi:10.1258/phleb.2010.010011.

[15] Moazzam Z, Yoo PB. Frequency-dependent inhibition of bladder function by saphenous nerve stimulation in anesthetized rats. Neurourol Urodyn 2017. doi:10.1002/nau.23323.

[16] Elder CW, Yoo PB. Co-activation of saphenous nerve fibers: a potential therapeutic mechanism of percutaneous tibial nerve stimulation?. In: Proceedings of the 2016 IEEE 38th annual international conference of the engineering in medicine and biology society (EMBC). Orlando, Florida; 2016.

[17] Kuhn A, Keller T, Lawrence M, Morari M. A model for transcutaneous current stimulation: simulations and experiments. Med Biol Eng Comput 2009;47:279–89. doi:10.1007/s11517-008-0422-z.

[18] Ellis H, Logan BM, Dixon AK. Human sectional anatomy. (3rd Ed). Hodder Arnold; 2007.

[19] Fukunaga T, Roy RR, Shellock FG, Hodgson JA, Day MK, Lee PL, et al. Physiological cross-sectional area of human leg muscles based on magnetic resonance imaging. J Orthop Res 1992;10:928–34. doi:10.1002/jor.1100100623.

[20] Sabetian P, Popovic MR, Yoo PB. Optimizing the design of bipolar nerve cuff electrodes for improved recording of peripheral nerve activity. J Neural Eng 2017;14. doi:10.1088/1741-2552/aa6407.

[21] Yoo PB, Durand DM. Selective recording of the canine hypoglossal nerve using a multicontact flat interface nerve electrode. IEEE Trans Biomed Eng 2005;52:1461–9. doi:10.1109/TBME.2005.851482.

[22] Grinberg Y, Schiefer MA, Tyler DJ, Gustafson KJ. Fascicular perineurium thickness, size, and position affect model predictions of neural excitation. IEEE Trans Neural Syst Rehabil Eng 2008;16:572–81. doi:10.1109/TNSRE.2008.2010348.

[23] Gabriel S, Lau RW, Gabriel C. The dielectric properties of biological tissues: III. Parametric models for the dielectric spectrum of tissues. Phys Med Biol 1996;41:2271–93.

[24] Rattay F. Analysis of models for external stimulation of axons. IEEE Trans Biomed Eng 1986;33:974–7. doi:10.1109/TBME.1986.325670.

[25] Danner SM, Hofstoetter US, Ladenbauer J, Rattay F, Minassian K. Can the human lumbar posterior columns be stimulated by transcutaneous spinal cord stimulation? a modeling study. Artif Organs 2011;35:257–62. doi:10.1111/j.1525-1594.2011.01213.x.

[26] McIntyre CC, Richardson AG, Grill WM. Modeling the excitability of mammalian nerve fibers: influence of afterpotentials on the recovery cycle. J Neurophysiol 2002;87:995–1006. doi:10.1152/jn.00353.2001.

[27] McIntyre CC, Grill WM. Extracellular stimulation of central neurons: influence of stimulus waveform and frequency on neuronal output. J Neurophysiol 2002;88:1592–604.

[28] Boyd IA, Davey MR. Composition of peripheral nerves. London: E&S Livingston, Ltd.; 1968.

[29] Hursh JB. Conduction velocity and diameter of nerve fibers. Am J Physiol 1939;127:131–9.

[30] De Andrés J, Sala-Blanch X, De Andres J, Sala-Blanch X, De Andrés J, Sala-Blanch X. Peripheral nerve stimulation in the practice of brachial plexus anesthesia: a review. Reg Anesth Pain Med 2001;26:478–83. doi:10.1053/rapm.2001.26485.

[31] Ford DJ, Pither C, Raj PP. Comparison of insulated and uninsulated needles for locating peripheral nerves with a peripheral nerve stimulator. Anesth Analg 1984;63:925–8.

[32] Yoo P, Grill W. Minimally-invasive electrical stimulation of the pudendal nerve: a pre-clinical study for neural control of the lower urinary tract. Neurourol Urodyn 2007;569:562–9 doi:10.1002/nau.

[33] Sauter AR, Dodgson MS, Kalvøy H, Grimnes S, Stubhaug A, Klaastad Ø. Current threshold for nerve stimulation depends on electrical impedance of the tissue: a study of ultrasound-guided electrical nerve stimulation of the median nerve. Anesth Analg 2009;108:1338–43. doi:10.1213/ane.0b013e3181957d84.

[34] McGuire EJ, Zhang SC, Horwinski ER, Lytton B, Shi-chun Z, Horwinski ER, et al. Treatment of motor and sensory detrusor instability by electrical stimulation. J Urol 1983;129:78–9.

[35] Peters KM, Carrico DJ, Perez-Marrero RA, Khan AU, Wooldridge LS, Davis GL, et al. Randomized trial of percutaneous tibial nerve stimulation versus sham efficacy in the treatment of overactive bladder syndrome: results from the sumit trial. J Urol 2010;183:1438–43. doi:10.1016/j.juro.2009.12.036.